Food & Function

ROYAL SOCIETY OF CHEMISTRY

PAPER

View Article Online
View Journal | View Issue

Cite this: *Food Funct.*, 2026, **17**, 1817

Metabolomic analysis reveals novel ethylated hydroxytyrosol metabolites in colon cancer cells

Clara Noguera-Navarro, [a] Carlos J. García, [b] David Auñón, [c] Ángel Gil-Izquierdo [b] and Silvia Montoro-García *[a]

Plants produce a diverse array of secondary metabolites, with hydroxytyrosol (HT) and its derivatives distinguished by their antioxidant and chemopreventive properties. Upon dietary consumption, native HT undergoes extensive biotransformation, initially facilitated by the gut microbiota. Increasing evidence suggests that several of these downstream products, rather than the parent molecule, are responsible for the most significant biological effects in mammalian cells. The identification of novel metabolites may reveal unknown metabolic pathways, more particularly in distinct pathological contexts such as cancer. The *in vitro* simulated gastrointestinal digestion (INFOGEST method) of HT, followed by bioavailability in the tumoral metabolically active intestinal Caco-2 cells (50 μM HT for 2, 4, and 6 h), was performed. Subsequently, an untargeted metabolomic analysis on the supernatant revealed novel HT-derived entities compared with water. Among these, ethoxy phenylacetic acid sulfates (4, 5), ethyl hydroxyphenylacetate acid sulfate (6) and ethoxy hydroxyphenylacetic acid or ethyl hydroxyphenylacetate glucuronide were described for the first time in a study and confirmed by MS/MS fragmentation. These accumulated ethylated forms were undetectable in non-tumoral plasma samples from HT-supplemented humans (60 mg day^{-1} HT for 28 days) and mice (50 mg kg^{-1} day^{-1} HT for 2 months), suggesting a tumour-specific or, at the very least, tumour-favoured biotransformation pathway. These findings not only expand the diversity of HT metabolites but also propose ethoxy-phenylacetic acid and its sulfate conjugate as potential biomarkers for cancer detection.

Received 29th September 2025,
Accepted 12th January 2026

DOI: 10.1039/d5fo04197j

rsc.li/food-function

Introduction

Plants produce polyphenols as secondary metabolites. Hydroxytyrosol (HT, 3,4-dihydroxyphenyl-ethanol), a phenolic acid from extra virgin olive oil (EVOO), has long been recognised as a potent anti-inflammatory, anti-proliferative and anti-antioxidant monophenol for the prevention of non-communicable diseases, such as cardiovascular diseases and cancer.[1–3] In 2011, the European Food Safety Authority (EFSA) approved a health claim stating that 5 mg per day of HT has beneficial effects.[4] Its simple and small chemical polar structure ($C_8H_{10}O_3$) hinders its bioavailability, especially in the small intestine, and raises questions about how it can exert the beneficial effects reported to date.[1] Subsequent modifications, such as the formation of oleuropein and its hydrolysis, lead to different forms: free, acetate and complexed or esterified with other compounds.[5] Indeed, free HT can barely be detected in plasma 1 h after consumption.[1] The lipophilic derivatives (secoiridoids), together with their formulation in matrices and oils, have been shown to increase their absorption and stability[6,7] as well as target-specific cell survival and proliferation pathways.[8]

Upon consumption, the original form of HT is modified by the microbiota, cellular metabolic pathways and the liver into distinct metabolites with wide pharmacokinetic characteristics. Emerging evidence indicates that the gut microbiota plays a crucial role in the modification of HT into secondary metabolites with enhanced potential anticancer properties, which may contribute to the protective effects of EVOO consumption against colorectal cancer.[9,10] Indeed, several studies have demonstrated that HT induces alterations in human colon cancer cells but not in normal colon epithelial cells, such as apoptosis[11] or DNA methylation.[12] Subsequently, human metabolism mainly occurs in the liver (glucuronidation, sulfation, *etc.*).[13] A list of well-known metabolites has been identified in plasma, such as hydroxytyrosol-3-glucuro-

[a]*Preclinical Research of Bioactive Compounds and Drugs (PREBIOF), Izpisúa Lab HiTech, Faculty of Health Sciences, Universidad Católica de Murcia (UCAM), Campus los Jerónimos, 30107 Murcia, Spain. E-mail: smontoro@ucam.edu; Tel: +34 968278725*
[b]*Quality, Safety, and Bioactivity of Plant Foods Group, Department of Food Science and Technology, CEBAS-CSIC, University of Murcia, 30100 Murcia, Spain*
[c]*Molecular Recognition and Encapsulation Research Group (REM), Health Sciences Department, Universidad Católica de Murcia (UCAM), Campus los Jerónimos, 30107 Murcia, Spain*

nide, homovanillic acid (HVA) and hydroxytyrosol-3-sulfate.[14] At the *in vitro* level, HT esters (HT acetate), HT alkyl ethers, HT analogues, HT thio-derivatives (thioacetate, thiol, and disulfide groups), and HT-derived isochromans have also been identified.[15] Furthermore, their vast structural diversity and potential modifications under normal and pathological conditions[16,17] challenge their identification, quantification and estimation of the recommended dietary intake. Metabolomics is useful for the sensitive detection of small molecules and high-resolution quadrupole time-of-flight (HR-Q-TOF) attempts to complement classical targeted metabolomics. Both techniques have been employed not only to characterize pathways under normal conditions but also to identify novel markers based on tumor biology.[18]

For a compound to exert its effects in normal and disease states, its bioavailability is essential. This study aimed to examine the HT metabolome using untargeted metabolomics and confirm the findings with UV analysis on colorectal cancer cells. In addition, it sought to investigate new metabolites present in the plasma of healthy individuals (humans and mice). Metabolomics holds promise for identifying a wide range of secondary HT intermediates that may be linked to antitumor properties.

Materials and methods

In vitro digestion of hydroxytyrosol

Hydroxytyrosol with a purity exceeding 99% was chemically synthesised by Seprox Biotech, SL. (Murcia, Spain). A digestion assay for HT was performed following the protocol described by Minekus *et al.*[19] Briefly, simulated fluids were prepared to a final volume of 500 mL. The composition of each fluid was as follows: simulated salivary fluid (SSF) contains 15.1 mL KCl (37.3 g L^{-1}), 3.7 mL KH_2PO_4 (68 g L^{-1}), 6.8 mL $NaHCO_3$ (84 g L^{-1}), 0.5 mL $MgCl_2(H_2O)_6$ (30.5 g L^{-1}), 0.06 mL $(NH_4)_2CO_3$ (48 g L^{-1}) and HCl (6 mol L^{-1}) to adjust the pH to 7.0; simulated gastric fluid (SGF) contains 6.9 mL KCl (37.3 g L^{-1}), 0.9 mL KH_2PO_4 (68 g L^{-1}), 12.5 mL $NaHCO_3$ (84 g L^{-1}), 11.8 mL NaCl (117 g L^{-1}), 0.4 mL $MgCl_2(H_2O)_6$ (30.5 g L^{-1}), 0.5 mL $(NH_4)_2CO_3$ (48 g L^{-1}) and HCl (6 mol L^{-1}) to adjust the pH to 3.0; and simulated intestinal fluid (SIF) contains 6.8 mL KCl (37.3 g L^{-1}), 0.8 mL KH_2PO_4 (68 g L^{-1}), 85 mL $NaHCO_3$ (84 g L^{-1}), 38.4 mL NaCl (117 g L^{-1}), 0.33 mL $MgCl_2(H_2O)_6$ (30.5 g L^{-1}) and HCl (6 mol L^{-1}) to adjust the pH to 7.0.

The entire digestion process was performed at 37 °C, and all samples were prepared in triplicate. The procedure was as follows: 5 mL of water (control) or the HT sample (2 g L^{-1}) was added to a mixture containing 3.5 mL of SSF, 0.5 mL of saliva amylase (1500 U mL^{-1} SSF dissolved), 25 μL of $CaCl_2$ (0.3 M) and 975 μL of distilled water. The final 10 mL mixture was incubated for 2 minutes. The 10 mL bolus was mixed with 7.5 mL of SGF, 16 mL of porcine pepsin (25 000 U mL^{-1} SGF dissolved), 0.5 μL of $CaCl_2$ (0.3 M), 0.2 mL of HCl (1 M) and 695 μL of distilled water, reaching a final volume of 20 mL. This mixture was incubated at 37 °C for 2 hours. Finally, the resulting 20 mL gastric chyme was combined with 11 mL of SIF, 5 mL of a pancreatin solution (800 U mL^{-1} SFI based), 2,5 mL of fresh bile (160 mM), 40 μL of $CaCl_2$ (0.3 M), 0.5 mL of NaOH (1 M) and 1.31 mL of distilled water.

At the end of each digestion phase, samples were collected in triplicate. The samples were centrifuged at 4000*g* for 25 minutes at 4 °C and then frozen at −80 °C for future analysis.

Cell viability assay for hydroxytyrosol treatment

Caco-2 cells (ATCC HTB-37) were seeded at a concentration of 30 000 cells per well in 96-well plates and then incubated at 37 °C for 24 hours. Subsequently, they were treated with increasing concentrations of HT (1–1000 μM). The treatment was incubated at 37 °C for another 24 hours. Subsequently, 30 μL of thiazolyl blue tetrazolium bromide (MTT) at a concentration of 1.9 mg mL^{-1} was added, followed by a 4-hour incubation at 37 °C in the dark. The medium was then aspirated, and 200 μL of dimethyl sulfoxide (DMSO) per well was added, with a 30-minute incubation at room temperature under orbital agitation. Finally, the plate was measured at 570 nm with a reference wavelength of 620 nm. A non-toxic HT concentration of 50 μM was used for the bioavailability study.

Quantification of hydroxytyrosol and bioavailability assay

The HT content was quantified for further bioavailability assay *via* high-performance liquid chromatography (HPLC, Agilent 1200, Germany) equipped with a diode array detector. A C18 Polaris column (150 × 4.6 mm, 5 mm) was maintained at 35 °C. The mobile phase consisted of 0.1% formic acid (A) and methanol (B), applied under a gradient elution program (0.0 min 10% B, 5.0 min 30% B, 17.5 min 100%, 20 min 100% B, 30.0 min 10% B, 35 min 10%).[2] Before analysis, a calibration curve was created using a standard HT sample (Phyproof ® ≥ 90%; reference substance, PhytoLab) through serial 1 : 2 dilutions from a stock solution (25 mg in 100 mL of the initial solvent mixture). HT was identified at a retention time of 4.846 min and quantified using a calibration curve ranging from 250 to 7.8 mg L^{-1}.[20]

A 24-well plate with Transwell™ inserts was used to seed 300 000 Caco-2 cells (ATCC HTB-37) per well. This cell line is derived from colorectal adenocarcinoma and maintains metabolic features characteristic of tumoral cells. The cells were incubated for 20–21 days to allow the formation of a differentiated epithelium. During this period, the culture medium was replaced every 48 hours with complete DMEM with L-gutamine, 10% fetal bovine serum (FBS) and penicillin/streptomycin (P/S) to ensure optimal cell development.

Once confluence was reached, transepithelial electrical resistance (TEER) was measured using an ERS-2 (MiliCell®) resistance system. The epithelial monolayer was considered established when all wells exhibited resistance values above 800 Ω, indicating tight junctions.[21] Experimental conditions, control (water digestion) and 50 μM HT, previously quantified from the *in vitro* digestion processes, were added to the apical side. Each experimental condition was performed in duplicate,

at different time points (2, 4 and 6 hours). Aliquots from time 0 hours were collected as basal references. At the end of each incubation period, apical and basal supernatants were recollected from the Transwell™ system. These samples were centrifuged to remove unwanted suspended material, preserving only the supernatant containing free particles. Finally, the supernatants were frozen at −80 °C for further analysis.

Plasma samples

Human plasma samples were obtained by venipuncture from two patients at a high cardiovascular risk after intake of 60 mg day^{-1} of HT for 28 days.[20] This concentration is equivalent to the intake of four caramels per day, each containing 15 mg of HT complexed with β-cyclodextrins, taken between meals. Blood samples were collected at the initial point and after 28 days of HT consumption in EDTA vacutainer tubes. The human study was approved by the Ethical Committee of the Catholic University of Murcia, Spain (CE042213, Clinical Trials ID: NCT06319417).[20]

An animal study was also conducted, which involved two 5-week-old athymic nude mice (Crl: NU(NCr)-Foxn1nu, Charles River, France). During the 2-month period, HT dissolved in water (50 mg kg^{-1} day^{-1}) was administered *via* oral gavage 5 days per week in volumes of 60–100 μL. This dosage is suitable for mice weighing 20–30 g. The animal study was approved by the Ethical Committee of *Instituto Murciano de Investigación Biosanitaria* (No. A13240502). Mice plasma samples were obtained *via* terminal intracardiac blood collection performed under anaesthesia using a mixture of fentanyl (0.075 mg kg^{-1}), midazolam (7.5 mg kg^{-1}), and medetomidine (0.75 mg kg^{-1}) dissolved in sterile saline. Death was confirmed by cervical dislocation.

Metabolite extraction

Metabolite extraction involved mixing three parts of each sample with one part of an acetonitrile/formic acid (98 : 2) mixture, followed by vortexing for 2 minutes. Subsequently, the mixture was placed in a bath sonicator for 10 minutes. Finally, the samples were centrifuged at 4000*g* for 20 minutes, and the final supernatant was collected. Next, samples were evaporated in a SpeedVac (Savant SPD121P, Thermo Scientific, Alcobendas, Spain) at room temperature. Dry samples were reconstituted with 200 μL of methanol and transferred to glass vials for analysis. Acetonitrile and water 0.1% (v/v) formic acid were purchased from J.T. Baker (Deventer, the Netherlands), and formic acid was obtained from Panreac (Barcelona, Spain).

Untargeted metabolomic analysis *via* UHPLC-ESI-QTOF-MS

Untargeted metabolomics analysis was conducted using a U-HPLC system (Infinity 1290; Agilent) coupled with a high-resolution quadrupole time-of-flight mass spectrometer (6550 iFunnel Q-TOF LC/MS; Agilent) equipped with an Agilent Jet Stream (AJS) electrospray ionisation (ESI) source. The mass spectrometer operated in the negative ion mode under the following conditions: gas temperature of 150 °C, drying gas flow at 14 L min^{-1}, nebulizer pressure set at 40 psig, sheath gas temperature of 350 °C, sheath gas flow at 11 L min^{-1}, capillary voltage of 3500 V, fragmentor voltage of 120 V, and octapole radiofrequency voltage of 750 V. Data acquisition was performed across an *m*/*z* range of 50–1700 at a scan rate of 3 spectra per second, with real-time mass correction using reference ions at *m*/*z* 112.9855 and 1033.9881.

The MS/MS spectra of target product ions were acquired within an *m*/*z* range of 100–1100, applying a retention time window of 1 min, collision energy varying from 5 to 60 eV, and a scan rate of 1 spectrum per second. Chromatographic separation was performed on a reversed-phase C_{18} column (Poroshell 120, 3 × 100 mm, 2.7 μm pore size) maintained at 30 °C. The mobile phase consisted of water with 0.1% formic acid (Phase A) and acetonitrile with 0.1% formic acid (Phase B), with a flow rate of 0.4 mL min^{-1}. The analytes were eluted using the following gradient: 0 min, 1% B; 10 min, 82% B; 16 min, 62% B; 22 min, 5% B; 24 min, 5% B; 25–30 min, 1% B.

Targeted metabolomics using UV spectra characterization *via* HPLC-DAD-ESI-MS/MS (IT)

The identification of new HT derivatives was performed using an Agilent 1100 HPLC system equipped with a photodiode array detector (G1315D) and coupled in series to an HCT Ultra Bruker Daltonics ion trap mass spectrometer *via* an electrospray ionisation (ESI) interface (HPLC-DAD-ESI-MS/MS-IT). Chromatographic separation was performed on a Poroshell 120 EC column (3 × 100 mm, 2.7 μm) from Agilent Technologies (Waldbronn, Germany). The mobile phases consisted of water/formic acid (99 : 1, v/v) (Phase A, Panreac, Barcelona, Spain) and acetonitrile (Phase B, J.T. Baker, Deventer, the Netherlands). The following gradient was applied: 0 min, 1% B; 10 min, 82% B; 16 min, 62% B; 22 min, 5% B; 24 min, 5% B; 25–30 min, 1% B. The flow rate was maintained at 0.4 mL min^{-1}, with an injection volume of 10 μL and a column temperature of 25 °C. UV spectra were recorded in the 200–600 nm range.

For mass spectrometry analysis, the electrospray source ionisation (ESI) was operated under the following conditions: nebuliser pressure, 65 psi; dry gas flow, 11 L min^{-1}; and dry gas temperature, 350 °C. The capillary voltage was set to 4 kV, and data were acquired in the negative ion mode across an *m*/*z* range of 100–1500, with a target mass of 500. The targeted MS/MS mode was used, applying a fragmentation amplitude of 1 V for ion isolation and fragmentation of the selected ions.

Data processing

Data acquisition was performed in the centroid and profile modes. The raw data were converted into the .abf format and processed using MS-DIAL 5.1.2 (prime.psc.riken.jp/compms) to generate data matrices. Feature extraction parameters were optimised to comprehensively cover the metabolome of the samples. Data collection was set with an MS1 tolerance of 0.01 Da, whereas peak detection parameters included a minimum peak abundance of 1000 and a mass window of 0.1 Da. For smoothing, a linearly weighted moving average method was

applied with a smoothing level of three scans. The generated data matrices were subsequently exported to the MetaboAnalyst platform (metaboanalyst.ca, Xia Lab) for evaluation and multivariate model generation. Before model creation, missing value imputation, abundance filtering, log transformation, and auto scaling were applied. After assessment of the multivariate models, a pattern-hunting analysis was conducted based on the presence of HT-sulfate. This step enabled the tentative identification of novel HT-derived molecules. After data processing, the tentatively identified derivatives were further analysed using MassHunter Qualitative 10.0 (version B.10.0, Agilent software metabolomics, Agilent Technologies, Waldbronn, Germany).

Statistical analyses

Principal component analysis (PCA), partial least-squares discriminant analysis (PLS-DA), heatmap analysis, and ANOVA simultaneous component analysis (ASCA) were performed using MetaboAnalyst (metaboanalyst.ca, Xia Lab) for untargeted analyses.

Results

Hydroxytyrosol decreases during the digestion phases

First, the HT concentration was quantified *via* HPLC in the distinct phases of the *in vitro* digestion, showing a progressive decrease (Fig. 1). The concentration was initially 1981 ± 1.8 mg L^{-1} (100%), but it dropped to 760 ± 1.9 mg L^{-1} (38.2% ± 0.9%) after the oral phase. The reduction from the oral to the gastric phase, resulting in a concentration of 554 ± 0.2 mg L^{-1} (28.1% ± 0.1%), was less pronounced than the initial decrease. Ultimately, a substantial reduction was observed in the intestinal phase, with the concentration reaching 74 ± 0.6 mg L^{-1} (4.0% ± 0.3%). It should be noted that a concentration of 2 g L^{-1} HT was used in the *in vitro* digestion to maximize analytical sensitivity and ensure reproducibility, rather than to mimic dietary exposure.

Multivariate analysis results

After confirming Caco-2 cell viability at 50 μM HT (SI Fig. S1), samples from the *in vitro* digestion and bioavailability assays were collected, extracted and analysed *via* UPLC-ESI-QTOF-MS. After preprocessing the raw data, a total of 67 435 entities were aligned and used to create the data matrix. After removing the entities present in the control samples (water digestion), a final data matrix consisting of 36 365 entities was exported to MetaboAnalyst for evaluation. A PLS-DA model of a part of the dataset was created for VIP (Variable Importance in Projection) inspection. The PLS-DA model incorporated the basal and apical measured samples after 2 and 6 h of absorption (SI Fig. S1A). The PLS-DA explained a total of 37.1% of the data variability. The variables explained by component one separated the samples according to the region, whereas component two separated the samples according to the time. Once the multivariate model was evaluated and validated, HT-sulfate (233.01329_5.654) was identified as one of the most important entities in the PLS-DA model (VIP score = 3.30) (SI Fig. S1B) and was used to generate the pattern hunter (SI Fig. S1C). After the pattern hunter application, 106 candidates exhibiting the same pattern as HT-sulfate were identified.

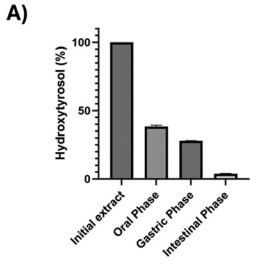

B)

Digestion Phase	Mean	SD
Oral Phase (mg/L)	760	±1.9
Gastric Phase (mg/L)	554	±0.2
Intestinal Phase (mg/L)	74	±0.6

Fig. 1 Hydroxytyrosol measurement using HPLC. (A) Percentage and (B) concentration in mg L^{-1} following simulated digestion at the oral, gastric and intestinal phases.

Metabolomics results

Based on the multivariate analysis results, nine molecules were tentatively identified as HT derivatives, four of which were reported for the first time (Table 1) *via* UHPLC-ESI-QTOF-MS. The rest of the tentative entities were reserved to be investigated in future research. HT-sulfate (**1**), HVA sulfate 1 (**2**), HVA sulfate 2 (**3**), ethoxy phenylacetic acid sulfate 1 (**4**), ethoxy phenylacetic acid sulfate 2 (**5**), ethyl hydroxyphenylacetate sulfate (**6**), HVA glucuronide 1 (**7**), HVA glucuronide 2 (**8**) and ethoxy hydroxyphenylacetic acid glucuronide or ethyl hydroxyphenylacetate glucuronide (**9**) were identified. The first six were confirmed by the MS/MS spectra. HT-sulfate, HVA sulfate and HVA glucuronide were previously identified.[22] On the other hand, the ethoxy phenylcetic acid sulfates (**4**, **5**), ethyl hydroxyphenylacetate sulfate (**6**) and ethoxy phenylacetic acid glucuronide or ethyl hydroxyphenylacetate glucuronide (**9**) were described for the first time in a previous study. According to the MS/MS fragmentation results, the three new isomers, ethoxy phenylacetic acid sulfates and ethyl hydroxyphenylacetate sulfate, were confirmed. They exhibited a fragmentation behaviour similar to those of HT sulfate and HVA sulfate, releasing the sulfate at 20 electron volts (eV) of collision energy and a fragment at *m*/*z* 195.0667. Furthermore, a fragment at *m*/*z* 232.0289 corresponding to the loss of the vinyloxy group was found to be the main fragment released at 20 eV (Fig. 2). This fragmentation pattern was observed at 20 and 30 eV, while 10 eV was not efficient to observe the main fragments. Furthermore, a fragment corresponding to HT was observed as the main fragment at 30 eV.

The three isomers, compounds (**4**), (**5**), and (**6**), presented the same fragmentation patterns. These results indicated that these new isomers present an ethyl group in the hydroxyl radicals. Unlike the previously described HT acetate sulfate,[23] which shows the same *m*/*z*, the fragmentation pattern of the derivatives observed in this study suggests that these new derivatives are distinct. This result indicates an *O*-ethoxylation

Table 1 Hydroxytyrosol intermediates detected by untargeted metabolomics

Compound	Formula	*m/z*	ppm	Rt	MS/MS fragments (neg polarity)	Collision E
(**1**) Hydroxytyrosol sulfate	$C_8H_{10}O_6S$	233.0137	3.87	5.63	153.0558; 123.0451	20
(**2**) Homovanillic acid sulfate 1	$C_9H_{10}O_7S$	261.0078	1.87	9.6	181.0505; 79.9570	20
(**3**) Homovanillic acid sulfate 2	$C_9H_{10}O_7S$	261.0069	1.97	9.89	181.0505; 79.9570	20
(**4**) Ethoxy phenylacetic acid sulfate 1	$C_{10}H_{12}O_7S$	275.0236	0.14	10.55	232.0285;248.0239;195.0661	20
(**5**) Ethoxy phenylacetic acid sulfate 2	$C_{10}H_{12}O_7S$	275.0233	−0.57	11.2	232.0234;248.0230;195.0665	20
(**6**) Ethyl hydroxyphenylacetate sulfate	$C_{10}H_{12}O_7S$	275.0233	−0.57	11.79	260.9330; 248.0234;195.0656	20
(**7**) Homovanillic acid glucuronide 1	$C_{15}H_{18}O_{10}$	357.0828	0.51	9.4	—	—
(**8**) Homovanillic acid glucuronide 2	$C_{15}H_{18}O_{10}$	357.0831	0.99	9.94	—	—
(**9**) Ethoxy phenylacetic acid glucuronide or ethyl hydroxyphenylacetate glucuronide	$C_{16}H_{20}O_{10}$		0.8	10.5	—	—

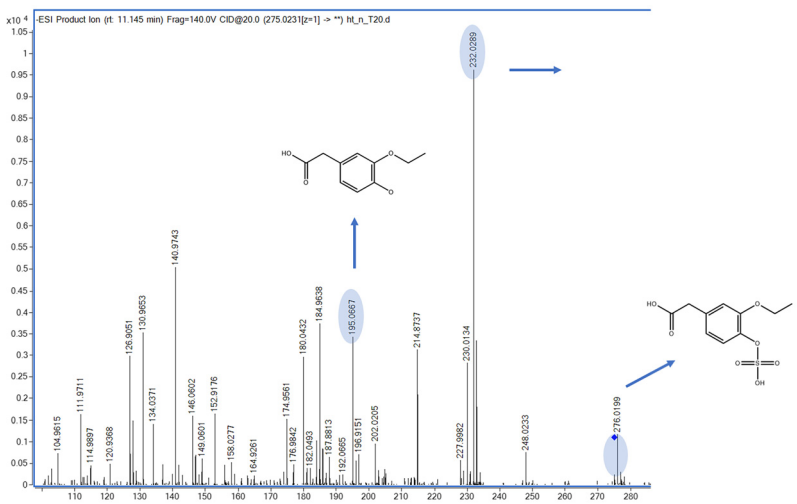

Fig. 2 MS/MS fragmentation pattern of the novel hydroxytyrosol derivatives. Fragmentation of ethoxy phenylacetic acid sulfate 2 (**5**) at 20 eV.

of either the hydroxyl or the carboxylic hydroxyl group, once the alcohol group is oxidized to an acid, as observed in the case of HVA (Fig. 3).

In addition, the new ethoxybenzene metabolites were measured by targeted UV spectra and ion trap MS/MS to confirm the fragmentation spectrum of these compounds by means of a discontinuous mass spectrometric measurement technique, which allows ion-by-ion isolation and thus unambiguous assignment of the association of the ionised compounds with the ionic fragments generated. Furthermore, the use of UV array detection in combination with MS/MS enabled correlation of these results with those obtained by the ion trap technology discussed above, which is an additional double confirmation of the ionic results obtained by UHPLC-ESI-QTOF-MS. In this way, the UV spectra of the phenol group of the HT-sulfate and the methoxybenzene present in the HVA sulfate were compared with the new metabolite to confirm the UV absorption of the benzene part and the differences between the methoxyl and ethoxyl groups. HT-sulfate, HVA-sulfate and ethoxy phenylacetic acid sulfate showed the same first absorption peak at 240 nm, corresponding to the benzene ring (Fig. 4). The –OH group in HT (Fig. 4A) and the $-OCH_3$ group in HVA (Fig. 4B) give rise to a second absorption band at 278 nm with similar intensity, as both substituents display strong electron-donating resonance effects that increase the electron density of the aromatic ring. This reinforcement of the $\pi \rightarrow \pi^*$ transition explains the high intensity of the 280 nm band, which is slightly more pronounced in the case of the phenolic –OH group.

In contrast, the $-OCH_2CH_3$ substituent of ethoxy phenylacetic acid sulfate (Fig. 4C) has a weaker resonance donation ability than methoxy and, therefore, contributes less to the enhancement of the 280 nm transition. As a result, the 280 nm band becomes noticeably less intense than the 240 nm band.

HPLC-DAD-ESI-MS/MS-IT only detected the most intense band as the precursor ion for fragmentation (ethoxy phenylacetic acid sulfate 1), as it is a less-sensitive technique than UHPLC-ESI-QTOF-MS. Although the ion intensity was not optimal for HPLC-DAD-ESI-MS/MS analysis, the results still revealed characteristic MS/MS fragments for all metabolites,

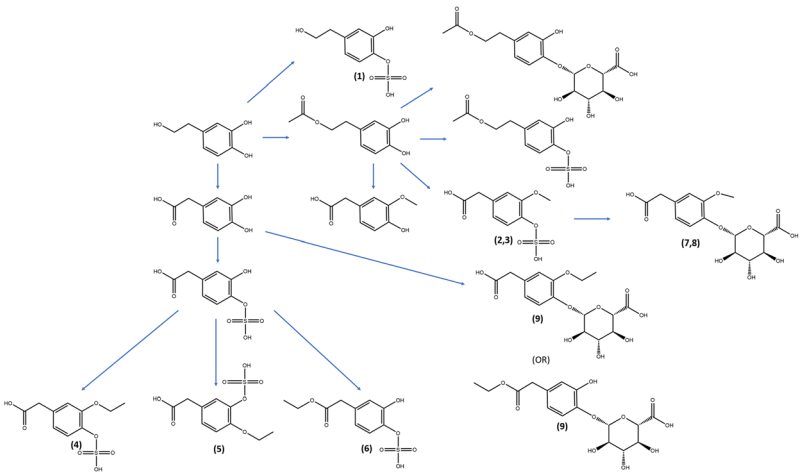

Fig. 3 Metabolic pathway proposed for hydroxytyrosol in colon cancer cells. Proposed chemical structures of the newly identified hydroxytyrosol-derived metabolites. (**1**) Hydroxytyrosol sulfate; (**2**) homovanillic acid sulfate 1; (**3**) homovanillic acid sulfate 2; (**4**) ethoxy phenylacetic acid sulfate 1; (**5**) ethoxy phenylacetic acid sulfate 2; (**6**) ethyl hydroxyphenylacetate sulfate; (**7**) homovanillic acid glucuronide 1; (**8**) homovanillic acid glucuronide 2; and (**9**) ethoxy phenylacetic acid glucuronide or ethyl hydroxyphenylacetate glucuronide.

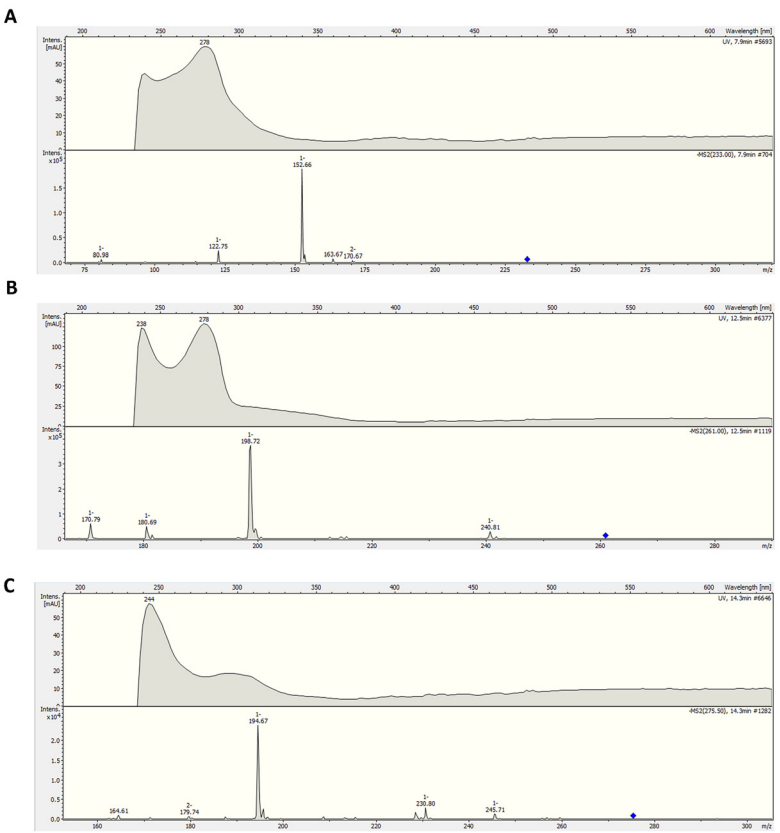

Fig. 4 Spectral UV absorption and MS/MS proposed fragmentation pattern of hydroxytyrosol derivatives. (A) Hydroxytyrosol sulfate (**1**); (B) homovanillic acid sulfate 1 (**2**); and (C) ethoxy phenylacetic acid sulfate 2 (**5**).

such as the loss of the sulfate group, yielding fragments at *m*/*z* 152, 180, and 195, respectively (Fig. 4A–C). In addition, a characteristic fragment at *m*/*z* 233, corresponding to the loss of the vinyloxy group, was also observed for ethoxy phenylacetic acid sulfate, as shown in the MS/MS analyses conducted using UHPLC-ESI-QTOF-MS (Fig. 4C).

Identification of ethoxy phenylacetic acid in plasma

The same methodology was applied to detect the presence of these new metabolites in plasma samples from non-tumoral conditions supplemented with high-dose HT. The ethylated derivatives were not detected in the plasma samples of humans and mice. According to previous pharmacokinetics studies of HT, the derivatives present the highest plasma levels between 30 min and 2 hours of HT intake.[24]

Discussion

Numerous studies have explored the influence of nutrition on the determination of risk and cancer progression.[25,26] Hydroxytyrosol and its metabolites have been extensively investigated in the literature[7,23,27] owing to their potential biological activity. As demonstrated in this study, the HT concentration significantly decreases during the digestive process. The HT metabolites can exert beneficial effects, such as antioxidant effects, on the organism,[27,28] and identifying unknown metabolites may reveal novel metabolic pathways of interest, more particularly in distinct pathological contexts such as cancer.

In this study, we evaluated *in vitro* and *in vivo* samples, identifying several metabolites, including the well-known HT-sulfate and HT-glucuronide.[29] HT-sulfate has been shown to function as an anti-inflammatory agent by reducing IL-1β levels,[30] whereas HT-glucuronide mitigates endoplasmic reticulum stress, thereby promoting atherosclerotic health.[31] In addition, HVA is of significant importance in this study, with the detection of its HVA-sulfate and HVA-glucuronide forms, as previously elucidated.[32] Although the metabolic properties of these forms have not been fully characterized, HVA has been identified as a potential modulator of depression[33] and a biomarker for diseases, such as neuroblastoma and neural crest tumors.[34] The molecular mechanisms and pharmacological activities of these identified metabolites remain to be fully elucidated, and several studies have shown that disease can influence polyphenol metabolism.[35,36]

Although numerous metabolites derived from HT have been extensively documented, this study identified novel ones, including ethoxy phenylacetic acid sulfate 1, ethoxy phenylacetic acid sulfate 2, ethyl hydroxyphenylacetate sulfate and ethoxy phenylacetic acid glucuronide or ethyl hydroxyphenylacetate glucuronide, with ethoxy phenylacetic acid sulfate 1 being the most abundant. Typically, phenolic compounds transform into other metabolites through processes such as methylation, carboxylation, sulfate conjugation, hydroxylation, and oxidation.[37] However, this study explored an unprecedented aspect, specifically the ethoxylation of HT, which has not been previously reported. It is established that ethanol is requisite for the formation of ethoxy groups by microorganisms specifically.[38–40] Nonetheless, in the current *in vitro* context, where no microbiota was present, this relevant modification still occurred in differentiated Caco-2 cells. Despite not being an *in vitro* proliferative tumor model, Caco-2 cells provide a suitable intestinal epithelial system for studying the tumoral metabolism of HT.

Moreover, the use of untargeted metabolomics, validated by UV analysis, demonstrates the power of this approach in identifying novel metabolites and physiological conditions.[41] Metabolomics examined *in vitro* samples lacking microbial presence but showing ethylations in tumoral cells. While the effects of ethylation on HT are not well established, such chemical modification can significantly alter its properties and biological activities. In cancer cells, aberrant ethoxylation can occur due to dysregulated enzymatic activity or altered metabolic processes.[42] These modifications may further affect proteins, lipids, and other biomolecules, potentially contributing to tumor progression and drug resistance. For instance, ethoxylation of certain proteins may alter their localization or interactions with other molecules, potentially promoting oncogenic signaling.[43,44] Understanding these specific ethoxylation pathways in tumoral cells may provide insights into cancer biology and potential therapeutic targets. To fully understand the effects of ethoxy-phenyl acetic acid sulfates 1–2 on tumor cell proliferation and viability, further research and specific experimental studies would be necessary. Our results indicate the potential biotransformation of HT in colon cancer cells; these ethoxylated metabolites can serve as potential biomarkers for colorectal cancer, pending further validation studies.[45]

To validate the presence of these newly identified metabolites under physiological conditions, we conducted the same analyses in *in vivo* systems, namely, human plasma samples and a mouse model supplemented with HT. The absence of these specific metabolites in plasma from patients and mice at risk for cardiovascular diseases does not conclusively prove that they were not produced by healthy conditions or that they are exclusively associated with tumoral processes. Indeed, other metabolites are rapidly cleared from the circulation in healthy individuals, and thus, the timing of sample collection could also have influenced the analysis.[46,47] Nonetheless, altered metabolism in tumoral processes may lead to increased production of ethoxylated metabolites, and further research, including other tumoral cell lines, colorectal cancer patients and time-course studies, would be necessary to establish a definitive link between these metabolites and tumoral processes.

This study provides novel insights into the *in vitro* formation of metabolites derived from HT; however, several limitations warrant consideration. The primary limitation is that the entire study was conducted under controlled conditions, which may not fully replicate the complexity of *in vivo* systems. As a result, the identified metabolites may differ in concentration, stability, or presence under other physiological conditions (as shown). Furthermore, the proposed enzymatic system remains theoretical and may require substantiation in future investigations. Finally, the absence of these molecules *in vivo* constrains our ability to conclude the pharmacokinetics, bioavailability, or biological activity of the detected metabolites in tumoral processes. Therefore, future studies should address these issues by validating the identified metab-

olites *in vivo* and exploring their biological functions and potential health effects.

Conclusions

This study provides valuable insights into the metabolic biotransformations of HT in tumoral colorectal cell samples using untargeted metabolomics. The study identified previously unreported ethylated HT metabolites, specifically ethoxy phenylacetic acid sulfates 1 and 2 and ethyl hydroxyphenylacetate sulfate in tumoral cells. The presence of ethoxylated metabolites in tumoral cells, but not in healthy plasma samples (human and mice), indicates potential tumor-specific metabolic processes. This finding opens new avenues for understanding cancer-specific metabolic alterations. Future research directions should focus on *in vivo* validation in animal models and human colorectal cancer patients and on the investigation of the proposed enzymatic pathways responsible for the ethylation of HT metabolites in tumoral cells. In conclusion, this study advances our understanding of HT metabolism in the context of cancer and highlights the potential of metabolomics in uncovering novel disease-specific metabolic processes. The confirmation of tumor-specific ethoxylated metabolites would open new possibilities for targeted therapies and diagnostic tools in cancer management.

Author contributions

Clara Noguera-Navarro: methodology, investigation, writing – original draft, writing – review, and editing. Carlos J. García: methodology, investigation, metabolomics, formal analysis, data curation, validation, writing – review, and editing. David Auñón: methodology and investigation. Ángel Gil-Izquierdo: methodology, investigation, metabolomics, and editing. Silvia Montoro-García: visualization, validation, resources, methodology, investigation, conceptualization, funding acquisition, project administration, writing – review, editing, and supervision.

Conflicts of interest

The authors declare that they have no known competing financial interests or personal relationships that could influence the work reported in this study.

Data availability

Further information and requests for resources and information should be directed to and will be fulfilled by Silvia Montoro-García (smontoro@ucam.edu). The data are accessible upon request. There are no restrictions on data access.

Supplementary information (SI) is available. See DOI: https://doi.org/10.1039/d5fo04197j.

Acknowledgements

CNN belongs to the Health Sciences PhD Program, Universidad Católica de Murcia (UCAM), Campus de los Jerónimos no. 135, Guadalupe 30107, Murcia, Spain and holds a PhD grant from the UCAM. This research was funded through the Project HIDROXITIR ("*Investigación de la bioactividad del hidroxitirosol y sus metabolitos en la prevención del cáncer*"), by PISTACIA INVESTIGACIONES, under the call "Financiación estructurada de proyectos de I + D por Agrupaciones de Interés Económico (A.I.E.)", in collaboration with INVENTIUM and by the Fundación Séneca de la Región de Murcia (JLI, Jóvenes Líderes en Investigación (22593/JLI/24)).

References

1 C. Noguera-Navarro, S. Montoro-García and E. Orenes-Piñero, Hydroxytyrosol: Its role in the prevention of cardiovascular diseases, *Heliyon*, 2023, **9**, e12963.
2 C. Vilaplana-Pérez, D. Auñón, L. A. García-Flores and A. Gil-Izquierdo, Hydroxytyrosol and potential uses in cardiovascular diseases, cancer, and AIDS, *Front. Nutr.*, 2014, **1**, 18.
3 Y. Lu, J. Zhao, Q. Xin, R. Yuan, Y. Miao, M. Yang, H. Mo, K. Chen and W. Cong, Protective effects of oleic acid and polyphenols in extra virgin olive oil on cardiovascular diseases, *Food Sci. Hum. Wellness*, 2024, **13**, 529–540.
4 EFSA Panel on Dietetic Products, Nutrition and Allergies (NDA), Scientific Opinion on the substantiation of health claims related to polyphenols in olive and protection of LDL particles from oxidative damage (ID 1333, 1638, 1639, 1696, 2865), maintenance of normal blood HDL cholesterol concentrations (ID 1639), maintenance of normal blood pressure (ID 3781), "anti-inflammatory properties" (ID 1882), "contributes to the upper respiratory tract health" (ID 3468), "can help to maintain a normal function of gastrointestinal tract" (3779), and "contributes to body defences against external agents" (ID 3467) pursuant to Article 13(1) of Regulation (EC) No 1924/2006, *EFSA J.*, 2011, **9**, 2033.
5 M. Robles-Almazan, M. Pulido-Moran, J. Moreno-Fernandez, C. Ramirez-Tortosa, C. Rodriguez-Garcia, J. L. Quiles and Mc. Ramirez-Tortosa, Hydroxytyrosol: Bioavailability, toxicity, and clinical applications, *Food Res. Int.*, 2018, **105**, 654–667.
6 A. Karković Marković, J. Torić, M. Barbarić and C. Jakobušić Brala, Hydroxytyrosol, Tyrosol and Derivatives and Their Potential Effects on Human Health, *Molecules*, 2019, **24**, 2001.
7 I. Kundisová, H. Colom, M. E. Juan and J. M. Planas, Pharmacokinetics of Hydroxytyrosol and Its Sulfate and Glucuronide Metabolites after the Oral Administration of Table Olives to Sprague-Dawley Rats, *J. Agric. Food Chem.*, 2024, **72**, 2154–2164.

8 S. Granados-Principal, J. L. Quiles, C. Ramirez-Tortosa, P. Camacho-Corencia, P. Sanchez-Rovira, L. Vera-Ramirez and M. C. Ramirez-Tortosa, Hydroxytyrosol inhibits growth and cell proliferation and promotes high expression of sfrp4 in rat mammary tumours, *Mol. Nutr. Food Res.*, 2011, **55**(Suppl 1), S117–S126.

9 L. Zhao, W. C. Cho and M. R. Nicolls, Colorectal Cancer-Associated Microbiome Patterns and Signatures, *Front. Genet.*, 2021, **12**, 787176.

10 R. Memmola, A. Petrillo, S. Di Lorenzo, S. C. Altuna, B. S. Habeeb, A. Soggiu, L. Bonizzi, O. Garrone and M. Ghidini, Correlation between Olive Oil Intake and Gut Microbiota in Colorectal Cancer Prevention, *Nutrients*, 2022, **14**, 3749.

11 L. Sun, C. Luo and J. Liu, Hydroxytyrosol induces apoptosis in human colon cancer cells through ROS generation, *Food Funct.*, 2014, **5**, 1909–1914.

12 A. del Saz-Lara, H. Boughanem, M. C. López de Las Hazas, C. Crespo, A. Saz-Lara, F. Visioli, M. Macias-González and A. Dávalos, Hydroxytyrosol decreases EDNRA expression through epigenetic modification in colorectal cancer cells, *Pharmacol. Res.*, 2023, **187**, 106612.

13 O. Khymenets, M. Fitó, S. Touriño, D. Muñoz-Aguayo, M. Pujadas, J. L. Torres, J. Joglar, M. Farré, M.-I. Covas and R. de la Torre, Antioxidant activities of hydroxytyrosol main metabolites do not contribute to beneficial health effects after olive oil ingestion, *Drug Metab. Dispos.*, 2010, **38**, 1417–1421.

14 G. Serreli, M. Le Sayec, C. Diotallevi, A. Teissier, M. Deiana and G. Corona, Conjugated Metabolites of Hydroxytyrosol and Tyrosol Contribute to the Maintenance of Nitric Oxide Balance in Human Aortic Endothelial Cells at Physiologically Relevant Concentrations, *Molecules*, 2021, **26**, 7480.

15 M. Robles-Almazan, M. Pulido-Moran, J. Moreno-Fernandez, C. Ramirez-Tortosa, C. Rodriguez-Garcia, J. L. Quiles and Mc. Ramirez-Tortosa, Hydroxytyrosol: Bioavailability, toxicity, and clinical applications, *Food Res. Int.*, 2018, **105**, 654–667.

16 Y. Song, M. Li, J. Liu, J. Wang, A. Zhou, Y. Cao, S. Duan and Q. Wang, Screening study of hydroxytyrosol metabolites from in vitro fecal fermentation and their interaction with intestinal barrier repair receptor AhR, *J. Food Sci.*, 2024, **89**, 10134–10151.

17 I. Domínguez-López, I. Parilli-Moser, A. Vallverdú-Queralt, A. Tresserra-Rimbau, C. Valls-Pedret, Z. Vázquez-Ruiz, O. Castañer, R. Estruch, E. Ros and R. M. Lamuela-Raventós, Microbial phenolic metabolites are associated with better frontal lobe cognition, *Food Sci. Hum. Wellness*, 2024, **13**, 3266–3272.

18 A. Zhang, H. Sun, G. Yan, P. Wang, Y. Han and X. Wang, Metabolomics in diagnosis and biomarker discovery of colorectal cancer, *Cancer Lett.*, 2014, **345**, 17–20.

19 M. Minekus, M. Alminger, P. Alvito, S. Ballance, T. Bohn, C. Bourlieu, F. Carrière, R. Boutrou, M. Corredig, D. Dupont, C. Dufour, L. Egger, M. Golding, S. Karakaya, B. Kirkhus, S. L. Feunteun, U. Lesmes, A. Macierzanka, A. Mackie, S. Marze, D. J. McClements, O. Ménard, I. Recio, C. N. Santos, R. P. Singh, G. E. Vegarud, M. S. J. Wickham, W. Weitschies and A. Brodkorb, A standardised static in vitro digestion method suitable for food – an international consensus, *Food Funct.*, 2014, **5**, 1113–1124.

20 C. Noguera-Navarro, K. T. Vinten, D. Auñón-Calles, C. Carazo-Díaz, G. E. Janssens and S. Montoro, Multi-omic analysis and platelet function distinguish treatment responses to hydroxytyrosol in cardiovascular risk, *Food Funct.*, 2025, **16**, 5928–5948.

21 S. Martínez-Sánchez, R. Domínguez-Perles, S. Montoro-García, J. A. Gabaldón, A. Guy, T. Durand, C. Oger, F. Ferreres and A. Gil-Izquierdo, Bioavailable phytoprostanes and phytofurans from *Gracilaria longissima* have anti-inflammatory effects in endothelial cells, *Food Funct.*, 2020, **11**, 5166–5178.

22 M. Schulz, F. Hübner and H.-U. Humpf, Evaluation of Food Intake Biomarkers for Red Bell Peppers in Human Urine Based on HPLC-MS/MS Analysis, *Mol. Nutr. Food Res.*, 2024, **68**, e2300464.

23 L. Rubió, A. Macià, R. M. Valls, A. Pedret, M.-P. Romero, R. Solà and M.-J. Motilva, A new hydroxytyrosol metabolite identified in human plasma: hydroxytyrosol acetate sulphate, *Food Chem.*, 2012, **134**, 1132–1136.

24 C. Alemán-Jiménez, R. Domínguez-Perles, S. Medina, I. Prgomet, I. López-González, A. Simonelli-Muñoz, M. Campillo-Cano, D. Auñón, F. Ferreres and Á. Gil-Izquierdo, Pharmacokinetics and bioavailability of hydroxytyrosol are dependent on the food matrix in humans, *Eur. J. Nutr.*, 2021, **60**, 905–915.

25 S. Vitale, E. Palumbo, J. Polesel, J. R. Hebert, N. Shivappa, C. Montagnese, G. Porciello, I. Calabrese, A. Luongo, M. Prete, R. Pica, M. Grimaldi, A. Crispo, N. Esindi, L. Falzone, V. Mattioli, V. Martinuzzo, L. Poletto, S. Cubisino, P. Dainotta, M. De Laurentiis, C. Pacilio, M. Rinaldo, G. Thomas, M. D'Aiuto, D. Serraino, S. Massarut, F. Ferraù, R. Rossello, F. Catalano, G. L. Banna, F. Messina, D. Gatti, G. Riccardi, M. Libra, E. Celentano, D. J. A. Jenkins and L. S. A. Augustin, One-year nutrition counselling in the context of a Mediterranean diet reduced the dietary inflammatory index in women with breast cancer: a role for the dietary glycemic index, *Food Funct.*, 2023, **14**, 1560–1572.

26 Y. Zhou, L. Teng, E. Ibáñez, H. Chen, A. Cifuentes and W. Lu, Application of Foodomics within the field of colorectal cancer prevention, diagnosis and treatment, *Food Funct.*, 2025, **16**, 6293–6312.

27 B. T. Martins, N. A. Faria, A. C. Macedo, M. Miragaia, A. T. Serra, M. R. Bronze and M. R. Ventura, Exploring the Biological Potential of Hydroxytyrosol and Derivatives: Synthetic Strategies and Evaluation of Antiproliferative, Antioxidant, and Antimicrobial Activities, *J. Agric. Food Chem.*, 2024, **72**, 26699–26710.

28 A. Atzeri, R. Lucas, A. Incani, P. Peñalver, A. Zafra-Gómez, M. P. Melis, R. Pizzala, J. C. Morales and M. Deiana,

Hydroxytyrosol and tyrosol sulfate metabolites protect against the oxidized cholesterol pro-oxidant effect in Caco-2 human enterocyte-like cells, *Food Funct.*, 2016, **7**, 337–346.

29 M. E. Sakavitsi, A. Breynaert, T. Nikou, S. Lauwers, L. Pieters, N. Hermans and M. Halabalaki, Availability and Metabolic Fate of Olive Phenolic Alcohols Hydroxytyrosol and Tyrosol in the Human GI Tract Simulated by the In Vitro GIDM-Colon Model, *Metabolites*, 2022, **12**, 391.

30 E. Terzuoli, G. Nannelli, A. Giachetti, L. Morbidelli, M. Ziche and S. Donnini, Targeting endothelial-to-mesenchymal transition: the protective role of hydroxytyrosol sulfate metabolite, *Eur. J. Nutr.*, 2020, **59**, 517–527.

31 E. Giordano, O. Dangles, N. Rakotomanomana, S. Baracchini and F. Visioli, 3-O-Hydroxytyrosol glucuronide and 4-O-hydroxytyrosol glucuronide reduce endoplasmic reticulum stress in vitro, *Food Funct.*, 2015, **6**, 3275–3281.

32 M. E. Sakavitsi, A. Breynaert, T. Nikou, S. Lauwers, L. Pieters, N. Hermans and M. Halabalaki, Availability and Metabolic Fate of Olive Phenolic Alcohols Hydroxytyrosol and Tyrosol in the Human GI Tract Simulated by the In Vitro GIDM-Colon Model, *Metabolites*, 2022, **12**, 391.

33 M. Zhao, Z. Ren, A. Zhao, Y. Tang, J. Kuang, M. Li, T. Chen, S. Wang, J. Wang, H. Zhang, J. Wang, T. Zhang, J. Zeng, X. Liu, G. Xie, P. Liu, N. Sun, T. Bao, T. Nie, J. Lin, P. Liu, Y. Zheng, X. Zheng, T. Liu and W. Jia, Gut bacteria-driven homovanillic acid alleviates depression by modulating synaptic integrity, *Cell Metab.*, 2024, **36**, 1000–1012.

34 M. Beals, B. Ramoo, C. Clinton Frazee and U. Garg, Quantitation of Neuroblastoma Markers Homovanillic Acid (HVA) and Vanillylmandelic Acid (VMA) in Urine by Gas Chromatography-Mass Spectrometry (GC/MS), *Methods Mol. Biol.*, 2022, **2546**, 185–194.

35 M. Á. Ávila-Gálvez, R. García-Villalba, F. Martínez-Díaz, B. Ocaña-Castillo, T. Monedero-Saiz, A. Torrecillas-Sánchez, B. Abellán, A. González-Sarrías and J. C. Espín, Metabolic Profiling of Dietary Polyphenols and Methylxanthines in Normal and Malignant Mammary Tissues from Breast Cancer Patients, *Mol. Nutr. Food Res.*, 2019, **63**, e1801239.

36 R. Zamora-Ros, L. Lujan-Barroso, D. Achaintre, S. Franceschi, C. Kyrø, K. Overvad, A. Tjønneland, T. Truong, L. Lecuyer, M.-C. Boutron-Ruault, V. Katzke, T. S. Johnson, M. B. Schulze, A. Trichopoulou, E. Peppa, C. La Vechia, G. Masala, V. Pala, S. Panico, R. Tumino, F. Ricceri, G. Skeie, J. R. Quirós, M. Rodriguez-Barranco, P. Amiano, M.-D. Chirlaque, E. Ardanaz, M. Almquist, J. Hennings, R. Vermeulen, N. J. Wareham, T. Y. N. Tong, D. Aune, G. Byrnes, E. Weiderpass, A. Scalbert, S. Rinaldi and A. Agudo, Blood polyphenol concentrations and differentiated thyroid carcinoma in women from the European Prospective Investigation into Cancer and Nutrition (EPIC) study, *Am. J. Clin. Nutr.*, 2021, **113**, 162–171.

37 Z. Gulsunoglu-Konuskan and M. Kilic-Akyilmaz, Microbial Bioconversion of Phenolic Compounds in Agro-industrial Wastes: A Review of Mechanisms and Effective Factors, *J. Agric. Food Chem.*, 2022, **70**, 6901–6910.

38 C. Löser, C. Kupsch, T. Walther and A. Hoffmann, A new approach for balancing the microbial synthesis of ethyl acetate and other volatile metabolites during aerobic bioreactor cultivations, *Eng. Life Sci.*, 2021, **21**, 137–153.

39 J. Podobiński, M. Zimowska, K. Samson, M. Śliwa and J. Datka, Ethoxy Groups on ZrO2, CuO, CuO/ZrO2 Al_2O_3, Ga2O3, SiO_2 and NiO: Formation and Reactivity, *Molecules*, 2023, **28**, 3463.

40 X. Li, X. Shen, J. Wang, H. I. Ri, C. Y. Mi, Y. Yan, X. Sun and Q. Yuan, Efficient biosynthesis of 3, 4-dihydroxyphenylacetic acid in *Escherichia coli*, *J. Biotechnol.*, 2019, **294**, 14–18.

41 S. Melnyk and R. Hakkak, Metabolic Status of Lean and Obese Zucker Rats Based on Untargeted and Targeted Metabolomics Analysis of Serum, *Biomedicines*, 2022, **10**, 153.

42 L. J. Yu, J. Matias, D. A. Scudiero, K. M. Hite, A. Monks, E. A. Sausville and D. J. Waxman, P450 enzyme expression patterns in the NCI human tumor cell line panel, *Drug Metab. Dispos.*, 2001, **29**, 304–312.

43 Z. Liu, M. Xiao, Y. Mo, H. Wang, Y. Han, X. Zhao, X. Yang, Z. Liu and B. Xu, Emerging roles of protein palmitoylation and its modifying enzymes in cancer cell signal transduction and cancer therapy, *Int. J. Biol. Sci.*, 2022, **18**, 3447–3457.

44 A. González-García, A. Garrido and A. C. Carrera, Targeting PTEN Regulation by Post Translational Modifications, *Cancers*, 2022, **14**, 5613.

45 L. Mezmale, M. Leja, A. M. Lescinska, A. Pčolkins, E. Kononova, I. Bogdanova, I. Polaka, I. Stonans, A. Kirsners, C. Ager and P. Mochalski, Identification of Volatile Markers of Colorectal Cancer from Tumor Tissues Using Volatilomic Approach, *Molecules*, 2023, **28**, 5990.

46 C. Bender, S. Strassmann and C. Golz, Oral Bioavailability and Metabolism of Hydroxytyrosol from Food Supplements, *Nutrients*, 2023, **15**, 325.

47 E. Miro-Casas, M.-I. Covas, M. Farre, M. Fito, J. Ortuño, T. Weinbrenner, P. Roset and R. de la Torre, Hydroxytyrosol disposition in humans, *Clin. Chem.*, 2003, **49**, 945–952.

